U. of Iowa 76-7

(NASA-CR-146508) OBSERVATIONS OF VELOCITY SHEAR DRIVEN PLASMA TURBULENCE (Iowa Univ.) 42 p HC $4.00 CSCL 03A

N76-19640

Unclas
G3/46 20632

Department of Physics and Astronomy
THE UNIVERSITY OF IOWA
Iowa City, Iowa 52242

U. of Iowa 76-7

Observations of Velocity Shear Driven Plasma Turbulence

by

P. M. Kintner, Jr.

February, 1976

Department of Physics and Astronomy
The University of Iowa
Iowa City, Iowa 52242

This research was supported in part by the National Aeronautics and Space Administration under Contract NAS1-11257 and Grant NGL-16-001-043 (97).

ABSTRACT

Electrostatic and magnetic turbulence observations from HAWKEYE-1 during the low altitude portion of its elliptical orbit over the southern hemisphere are presented. The magnetic turbulence is confined near the auroral zone and is similar to that seen at higher altitudes by HEOS-2 in the polar cusp. The electrostatic turbulence is composed of a background component with a power spectral index of $1.89 \pm .26$ and an intense component with a power spectral index of $2.80 \pm .34$. The intense electrostatic turbulence and the magnetic turbulence correlate with velocity shears in the convective plasma flow. Since velocity shear instabilities are most unstable to wave vectors perpendicular to the magnetic field, the shear correlated turbulence is anticipated to be two-dimensional in character and to have a power spectral index of 3 which agrees with that observed in the intense electrostatic turbulence.

I. INTRODUCTION

Plasma waves from 100 kHz to 1 Hz are a common feature of the high latitude ionosphere. In the ULF range, below the ion cyclotron frequency, waves and turbulence with both electric and magnetic components have been observed. One persistent feature is an electrostatic noise band below 500 Hz with a power law spectrum observed above 55° INV latitude peaking in intensity near the auroral zone and somewhat less intense over the polar cap [Kelly and Mozer, 1972; Barrington et al., 1971; Maynard and Heppner, 1969; Laaspere et al., 1971]. This noise band is frequently isotropic and propagates with a phase velocity small compared to the spacecraft velocity [Kelly and Mozer, 1972]. Narrow band electromagnetic waves have been observed near 100 Hz in the polar cusp and auroral oval [Gurnett and Frank, 1972]. At higher altitudes, 2 to 5 R_e, magnetic turbulence below 500 Hz with a f^{-4} spectrum is observed in the polar cusp [Russell et al., 1971; D'Angelo et al., 1974]. The presence of earthward streaming protons in the polar cusp [Frank, 1971] motivated D'Angelo [1973] to suggest that the parallel Kelvin-Helmholtz instability excited by velocity shear in the polar cusp proton flow is producing the magnetic turbulence.

A double cell convection pattern through the polar cap ionosphere has been established by Cauffman and Gurnett [1971] and Heppner

[1972]. At the center of each cell exists a surface across which the convection velocity reverses, frequently in a distance less than 100 km. Boundaries across which a velocity shear exist are susceptible to the transverse Kelvin-Helmholtz instability (for example, see Chandrasekhar, 1961). Typical magnetic Reynold's numbers of 10^3 to 10^4 for flow across the convection reversal also imply the flow should be turbulent. This report presents electric and magnetic wave measurements along with convection velocity measurements to establish the presence of turbulence at high latitudes and show that electrostatic power spectral indices agree with that predicted by hyrodynamic considerations [Kraichnan, 1967; Lilly, 1969].

II. INSTRUMENTATION

The HAWKEYE-1 spacecraft was launched into a highly elliptical orbit on June 3, 1974, with apogee over the north polar cap at 125,000 km and perigee near 500 km over the south polar cap. The orbital period is 49.94 hours and once every third orbit the spacecraft is tracked from Orroral, Australia, as the spacecraft crosses the southern hemisphere into the south polar cap. During this portion of the orbit ambient plasma densities are sufficiently large to permit operation of the static electric field meter [Kintner et al., 1976].

The electric antenna consists of a cylindrical dipole 42.25 meters from tip-to-tip. As the spin period of HAWKEYE-1 is 11.009 seconds, a static electric field measurement is made every 11 seconds. By assuming $\overline{E} \cdot \overline{B} = 0$, the complete electric field in the plane perpendicular to the local magnetic field is determined. Both components of the convection velocity perpendicular to the local magnetic field can then be calculated through $\overline{V}_c = \overline{E} \times \overline{B}/B^2$. The electric wave receivers have already been described by Kurth et al. [1975].

The magnetic wave sensor is a single search coil aligned parallel to the spacecraft spin axis. The search coil output is amplified and filtered by 8 channels from 1.7 Hz to 5.6 kHz which are shared with the electric receiver. The output of each filter is logarithmically compressed and telemetered with the electric measurements.

III. EXPERIMENTAL RESULTS

As HAWKEYE descends from apogee over the north polar cap it passes into the plasmasphere, through the magnetic equator, out of the plasmasphere, and, as it continues to lose altitude, over the auroral zone and polar cap. Figure 1 shows the response of the electric and magnetic VLF receivers during the descending node on Day 263, 1974, as the spacecraft travels from just south of the magnetic equator to the south polar cap. The output from 0 to 5 volts of each filter is shown on a logarithmic scale spanning 100 dB of amplitude.
At low L values, plasmasphere hiss between 178 Hz and 5.62 kHz is present in both the electric and magnetic receivers. The plasmaspheric hiss continues into the polar cap where escaping ray paths may exist [Muzzio and Angerami, 1972]. Starting at about 2242 UT VLF or auroral hiss is present at 1.7 kHz and 5.6 kHz in the electric and magnetic channels and continues until loss of telemetry at 2247 UT. Commencing at 2235 UT another feature can be distinguished in the 1.78 Hz through 56.2 Hz electric channels. This signal exhibits no magnetic component before 2243 UT, has a spectral density which decreases with increasing frequency, and peaks in intensity near the auroral zone. This signal is tentatively identified as the electrostatic noise band previously reported by Kelly and Mozer [1972] from OV1-17 at lower altitudes.

Although the 1.7 Hz to 56 Hz background electric noise before 2243 UT is contiguous to the intensification which extends to 178 Hz after 2243 UT, they are not necessarily otherwise identical. After 2243 UT the magnetic receiver responds from 1.7 Hz to 56 Hz coincidental to the increased amplitude of the electric signal. Over the auroral oval HAWKEYE commonly observes an electric and magnetic noise band between 1.7 and 56 Hz similar to that shown here on Day 263. The remainder of this paper concerns those electric and magnetic fluctuations.

A. Magnetic Signal

The spatial distribution of the magnetic noise band is presented in Figure 2. A survey of 47 passes into the southern polar cap were made by testing the 5.6 Hz magnetic channel for amplitudes above a threshold of 2 x 10^{-4} $gamma^2$/Hz. Except for the interval from 0600 MLT to 0900 MLT all 3 hour blocks of magnetic local time were nearly equally sampled. No telemetry coverage was available for HAWKEYE when in the cross hatched area. The equatorward border of the Feldstein K_p = 1 auroral oval is presented for comparison. The magnetic fluctuations occur at all local times. On the night side they correspond to the location of the auroral oval while on the day-side they extend both equatorward and poleward of the auroral oval. From 0600 MLT to 1800 MLT every pass for which telemetry coverage extends above 75° INV latitude observes the magnetic signal while on the night side roughly only half of the passes where coverage extends to 75° INV latitude observe a magnetic signal. Over the nightside polar cap there is an area where the signal is consistently less than 2×10^{-4} gamma^2/Hz.

Four spectral densities for the magnetic fluctuations between 2243 UT and 2245 UT are presented in Figure 3 for Day 263. The peak spectral densities of .3 to 3 gamma/$\sqrt{Hz}$ occur in the 1.7 Hz channel and decrease in amplitude to 4×10^{-4} gamma/$\sqrt{Hz}$ at 56 Hz. The spectrum is a power law and the magnetic power spectral indices are plotted in Figure 4 for 23 cases. The average value is 4.02 ± .59.

The magnetic spectrum is similar to that reported by D'Angelo [1974] when the HEOS-2 spacecraft is in the polar cusp at altitudes of 2-5 R_e. The hypothesis that at the HAWKEYE altitude of 2000 km these may be the same fluctuations was tested by examining low energy electron data from LEPEDEA to identify the polar cusp. In each case on the dayside, where the cusp could be identified, the polar cusp was found inside the region of magnetic fluctuations although the magnetic noise frequently extended one cusp width or more beyond each border of the polar cusp. The difference in north-south extent is the only one observed.

B. Electric Signal

The spatial distribution of the electric noise band is presented in Figure 5 for 47 passes into the south polar cap. Each dot represents one measurement exceeding a threshold of 2×10^{-10} V^2/m^2 Hz at 17 Hz and the dashed line corresponds to the plasmapause boundary for K_p = 2-4 [Carpenter, 1966]. The electric noise is uniformly distributed in local time and extends from 60° INV latitude to the poleward border of telemetry coverage. The threshold level is chosen to illustrate the low level background electric noise as well as the more intense electric noise. For example in Figure 1 the equatorward border of the 17 Hz electric noise defined by the threshold occurs at 2235 UT although the more intense noise is confined between 2243 UT and 2247 UT. If the threshold is increased to select the intense electric noise, the distribution would be similar to the magnetic noise illustrated in Figure 2. The equatorward border of the background electric noise agrees with the plasmapause location for K_p = 2-4.

Electric spectral densities for Day 263 are presented in Figure 6 for a period during the intense signal from 2244 UT to 2246 UT and for a period during the weaker background signal of 2240 UT to 2242 UT. Both spectra are approximately power laws but with different spectral indices. A spectrum of the form $P_E = E_o^2 f^{-a}$ was fit to 45 electric power spectrums. The results are divided into intense and background spectra by separating them at $E_o^2 = 2 \times 10^{-7}$ $V^2/m^2\sqrt{Hz}$. The histograms in Figure 7 clearly show the power spectral index to increase for more intense signals. Within each grouping there is no apparent relation between E_o^2 and a. The average power spectral indices are 2.80 ± .34 and 1.89 ± .26 for the intense and background signals respectively.

The parallel Kelvin-Helmholtz instability driven by a velocity shear in earthward streaming polar cusp protons has been suggested by D'Angelo <u>et al.</u> [1974] as the origin of magnetic fluctuations in the polar cusp. An alternative mechanism for the intense electric and magnetic noise on Day 263 is the transverse Kelvin-Helmholtz instability driven by the velocity shear in the convecting thermal magnetospheric plasma. The convective velocity field, calculated from the static electric field meter through the relation $\overline{V} = \overline{E} \times \overline{B}/B^2$, is plotted as vectors from the spacecraft position in magnetic invariant latitude and magnetic local time for Day 263, 1974, in Figure 8. Three regions of flow are present. Over the polar cap flow is primarily westward with an anti-sunward component. Between 76° INV and 68° INV latitude flow is primarily eastward with a small sunward component. Equatorward of 68° INV latitude the flow is weakly anti-sunward. The largest velocity shears occur between 2242 UT and 2247 UT.

Velocity shear is calculated from the change in consecutive velocity measurements divided by the distance the satellite moves between measurements ($|\overline{V}_n - \overline{V}_{n-1}|/|\overline{r}_n - \overline{r}_{n-1}|$). To measure $\overline{\nabla} \times \overline{V}_c$ exactly the spacecraft must be moving perpendicular to $\overline{\nabla} \times \overline{V}_c$ and to $\overline{V}_c$. If $\overline{V}_c$ is constant along a magnetic field line, $\overline{\nabla} \times \overline{V}_c$ will be parallel to the local magnetic field and as HAWKEYE is traveling nearly perpendicular to the local magnetic field and, from Figure 8, nearly perpendicular to the velocity field, only a slowly varying systematic error will be introduced. Both of these errors will decrease the measured shear. The quantity $|\overline{V}_n - \overline{V}_{n-1}|/|\overline{r}_n - \overline{r}_{n-1}|$ does not mix components of $\overline{\nabla} \cdot \overline{V}_c$ with $\overline{\nabla} \times \overline{V}_c$ since the magnetospheric plasma at this altitude is incompressible.

The shear for Day 263 is plotted in Figure 9. In the top panel are consecutive velocity measurements and in the lower two panels are the calibrated electric and magnetic power spectral densities. Velocity shear is plotted on a logarithmic scale in units of sec^{-1} and has a noise level of about 3×10^{-3} sec^{-1}. A broad peak in velocity shear is centered about 2244:30 UT and correlates very well with the intense electric and magnetic fluctuations.

Figure 10 shows a pass into the polar cap on Day 234 in the same format as Figure 9. Simultaneous electric and magnetic noise bands begin abruptly at 0054 UT coinciding with the abrupt increase in convective shear. This figure is presented to emphasize the repeatable nature of the correlation between convective velocity shear and the electric and magnetic fluctuations. On every occasion in which the static electric field meter is functioning and the shear exceeds 10^{-2} sec^{-1}, the electric and magnetic fluctuations are present and correlated with shear.

IV. DISCUSSION

The ULF signal reported here has both an electric and magnetic component although the noise band is not an electromagnetic plasma wave propagating in a cold plasma. If it were an electromagnetic wave the index of refraction (n = B/E) should not be a function of frequency below the ion cyclotron frequency. The local proton cyclotron frequency is about 350 Hz and, since the average electric spectral density is proportional to $f^{-1.4}$ while the average magnetic spectral density is proportional to f^{-2}, the index of refraction is proportional to $f^{-.6}$ instead of being constant. The distribution of noise will on either side of the polar cusp eliminate mechanisms where the waves propagate on the warm cusp plasma. As cold linear plasma theory cannot account for these fluctuations, other sources must be examined.

Field-aligned currents are a common feature of the auroral oval and their magnetic field must make some contribution to the magnetic fluctuations presented here. As HEOS 2 sampled a region much higher in altitude compared to HAWKEYE a test of the hypothesis that the magnetic fluctuations at both satellites are caused by field-aligned currents may be made by scaling the spectrums between the two altitudes. The magnetic spectra can be scaled between the two spacecraft assuming the field-aligned currents connect the two altitudes and do not disperse across field lines. Assume at HAWKEYE there is a distribution of current densities at position $\bar{r}$ with wave vector $\bar{k}$, $j(\bar{k},\bar{r})$. The magnetic field associated with that current density is proportional to

$$\Delta B_k \sim \frac{j(\bar{k},\bar{r})}{|\bar{k}|}$$

where $|\bar{k}| \sim \sqrt{B_o}$ and $j \sim 1/B_o$ along a flux tube. B_o is the local magnetic field. At HAWKEYE $B_o = 25{,}000\ \gamma$ and at HEOS $B_o = 300\ \gamma$. Associating subscript 1 with HAWKEYE and subscript 2 with HEOS, the magnetic spectra are related by

$$\Delta B_{k,1} = 7.6 \times 10^2\ \Delta B_{k,2}$$

The increased amplitude at lower altitudes arises solely from the convergent property of the earth's magnetic field. The measured frequency of a stationary structure with wave vector $\bar{k}$, through which a satellite is moving with velocity $\bar{V}$ is $f = \bar{V}\cdot\bar{k}$. A field aligned current confined to a flux tube will produce a signal whose frequency at HAWKEYE is related to the frequency at HEOS by $f_1/f_2 = V_1k_1/V_2k_2 = 36$ where $v_1 = 10$ km/sec and $v_2 = 2.5$ km/sec. The 20 Hz filter on HEOS should be compared with a 720 Hz signal at HAWKEYE and the signal at HAWKEYE should be 7.6×10^2 larger. Peak values reported for HEOS at 20 Hz vary from 10^{-3} to 10^{-2} gamma/$\sqrt{\text{Hz}}$ [D'Angelo, 1974]. Figure 11 shows 4 magnetic spectral densities made during peak amplitudes in the magnetic channel of HAWKEYE. Extrapolating to 700 Hz indicates the magnetic signal will be less than 10^{-4} gamma/$\sqrt{\text{Hz}}$ when it should be

700 times larger than the HEOS-2 magnetic signal if they are both caused by field-aligned currents confined to flux tubes.

D'Angelo et al. [1974] discuss the magnetic fluctuations at HEOS-2 as turbulence and notes that $\Delta B \cdot B_o/n \sim \Delta n/n$ is a constant for his measurements over different values of ΔB, B_o and n where n is the local number density. If the same process is occurring at HAWKEYE, $\Delta n/n$ should be the same as for HEOS-2 and ΔB can be scaled as a test of the mechanism. In this case

$$\frac{\Delta B_1}{\Delta B_2} = \frac{n_1}{n_2}\frac{B_{o,2}}{B_{o,1}} \cong .01\,\frac{n_1}{n_2}$$

The frequencies for a structure with the same wave vector scale with the spacecraft velocities only and hence $f_1 = 4\ f_2$. Using $f_2 = 20$ Hz again, the HEOS-2 spectra at 20 Hz should compare to HAWKEYE at 80 Hz. No reliable thermal plasma density measurements exist over the polar cap but, assuming say $n_1 = 10$ to $100\ n_2$, a range of values can be calculated as $\Delta B_1 = .1$ to $1\ \Delta B_2$. Extrapolating slightly to 80 Hz on Figure 11 the peak value is approximately 2×10^{-4} gamma/$\sqrt{\text{Hz}}$ which is .1 of the value observed at HEOS. The agreement of this scaling argument between satellites and the disagreement of the field-aligned current scaling arguments strongly suggest that the magnetic fluctuations are related to turbulence instead of being caused by field-aligned currents.

The latitudinal width of the magnetic fluctuations observed by HAWKEYE is frequently larger than would be expected by extending the

HEOS-2 observations earthward. This morphological difference may imply that the mechanisms exciting the turbulence are also different. If this is correct, the fully developed turbulent states originating from different linear mechanisms produce identical magnetic spectra which suggests that the turbulent state is in some respect independent of its origin.

The Kelvin-Helmholtz instability is capable of generating turbulence. For a review of linear instabilities driven by velocity shear see Gerwin [1968]. In space plasma linearly unstable fluid models have been used to investigate stability of the magnetopause [Southwood, 1968] and of the polar cusp [D'Angelo, 1972; D'Angelo <u>et al.</u>, 1974]. At the magnetopause a velocity shear exists between the magnetosheath plasma and the interior of the magnetosphere which is proposed to be responsible for generating pc2 to pc5 micropulsations. Lanzerotti <u>et al.</u> [1972] have pointed out that this mechanism should result in a frequency of occurrence null near noon which is not observed at L = 4. D'Angelo [1965] develops a model to account for turbulence observed in laboratory plasmas counter streaming along a magnetic field [D'Angelo and Goeler, 1966] and applies the model to polar cusp plasmas [D'Angelo, 1972]. Observation of magnetic fluctuations confined to the polar cusp at 2-5 R_e support this model but do not differentiate between shear in cusp plasmas streaming parallel to the local magnetic field and the shear in convective flow. None of those models predict what the final saturated states of the plasma are.

In hydrodynamic fluids turbulence in saturated nonlinear situations is better understood so I will use it to understand the signals presented here and their spectrums. In a three-dimensional fluid being stirred at wave vector k_o energy flows toward larger wave vectors. If a fluid is being excited at a sufficiently long wavelength, there will exist a range of wave vectors between k_o and the larger wave vectors where dissipation dominates. In this range the individual eddies are inertially dominated, and hence this is called the inertial subrange. Within the inertial subrange energy is transferred locally between states of different k by cascading towards larger wave vectors. Using the cascade process Kolmogoroff calculated the turbulent energy spectra in the inertially dominated subrange to have the form $\epsilon(k) = 4\pi k^2 |u(\vec{k})|^2 \sim k^{-5/3}$ where $u(\vec{k})$ is the velocity per unit mass at wave vector $\vec{k}$ of the fluid. (For a review of Kolmgoroff's theory see Batchelor, 1970). In two dimensions turbulence behaves much differently due to the formation of vortex cells. A two-dimensional fluid being stirred at k_o propagates energy to states of smaller wave vectors thus forming vortices and enstrophy to states of larger wave vectors where enstrophy is $k^2|u(k)|^2$. Kraichnan [1967] and Lilly [1969] show that a two-dimensional fluid being stirred at k_o has an energy spectrum $\epsilon(k) \sim k^{-5/3}$ for wave vectors smaller than k_o and $\epsilon(k) \sim k^{-3}$ for wave vectors larger than k_o but not extending to the viscous subrange.

Turbulence in a three-dimensional magnetic fluid will behave as a two-dimensional fluid if it is preferentially excited at wave vectors perpendicular to the magnetic field. In discussing velocity shear driven instabilities Chandrashekar [1961], and Hasegawa [1975], find a magnetic fluid to most unstable to wave vectors perpendicular to the magnetic field. Soucri [1975] has substantiated this using computer models. Hence in the region of large velocity shears magnetospheric turbulence will most likely be two dimensional.

The contribution of electric turbulence and magnetic turbulence to the fluid energy density at wave vector k may be calculated from $\bar{u} = \bar{E} \times \bar{B}/\bar{B}^2$. The first order contributions are $\bar{u}_k = \bar{E}_k \times \bar{B}/\bar{B}^2 - \bar{E} \times \bar{B}_k/\bar{B}^2$. By examining the electric and magnetic spectral densities the electric term is found to be much larger than the magnetic term assuming maximal geometry in both cases. The electrostatic power spectral density in k-space is thus directly proportional to the fluid spectral energy density, $E_k^{\,2} \sim 4\pi k^2 |u(\vec{k})|^2$.

The electric power spectral indices support the hypothesis that shear correlated electric field noise results from the spacecraft moving through a turbulent plasma. Kelly and Mozer [1962] have shown the phase velocity of this noise in the spacecraft reference frame to be equal to the spacecraft velocity. Hence the measured frequency is related to the spacecraft velocity by $\bar{k} \cdot \bar{V}_{s/c} = 2\pi f$ and the power spectral index in k-space is the same as in f-space if the power spectral density is isotropic and a power law. The measured index of $2.80 \pm .34$ in the large shear region agrees with that expected in the two-dimensional inertial subrange at wave vectors larger than those exciting the plasma. Outside the region driven by shear the power spectral index decreases to 1.89 ± .26 which includes the value 5/3 and suggests two alternative processes. Either the plasma is being two-dimensionally stirred at a wave length smaller than 100 m and energy propagates toward smaller wave vectors or as the turbulence propagates away from the shear driven region it no longer is oriented perpendicular to the magnetic field, thereby becoming three dimensionally turbulent. Energy then reverses its flow in k-space and procedes toward larger wave vectors with the spectral $\epsilon(k) \sim k^{-5/3}$.

The Kadomstev [1965] theory of ion acoustic turbulence (driven by electron currents) also implies a power spectrum of $\epsilon(k) \sim k^{-3}$. Since the intense electric noise and magnetic noise are also correlated, the magnetic signal might be interpreted as resulting from field aligned currents which then drive the electrostatic turbulence through Kadomstev's theory. The cusp, though, is embedded in the correlated electric and magnetic signals and is characterized by a plasma where $T_i \gg T_e$. Hence ion acoustic turbulence is strongly Landau damped over much of the area where the intense electrostatic signal is observed.

The velocity shear driven turbulence model may be further tested by examining the signal phase if it is elliptically polarized. The phase of magnetic vortices depend on the sign of the velocity derivative. An example is shown in Figure 12. A magnetic field line perturbed to oscillate about x_o in the x direction will acquire a velocity in the y direction such that it moves clockwise looking down the field line. If the sign of the velocity vectors are changed counterclockwise motion will occur. If coherent vortices can be individually examined their phase will provide a test of their origin. Although HAWKEYE cannot make phase measurements of the ULF noise presented here, ground based micropulsation stations do make phase measurements.

A common feature of convection over the polar cap is a reversal of convection velocity. For decreasing latitude equatorward of the reversal the velocities also decrease creating a region of approximately uniform shear. Poleward of the reversal the convection is not as uniform. Micropulsations from 1 mHz to 20 mHz observed by Samson et al. [1971] at high latitudes have the phase implied by shear in the high latitude convective velocity field equatorward of the reversal. During local morning they are polarized clockwise and during local evening they are polarized counterclockwise. Further they reverse phase near noon and change polarization across the approximate location of the electric field reversal.

V. SUMMARY AND CONCLUSIONS

Over the south polar cap near an altitude of 2000 km the HAWKEYE electric and magnetic receivers respond to ULF fluctuations. The magnetic ULF noise is located near the auroral oval although on the dayside it extends equatorward of the auroral oval. The electric ULF noise fills the volume sampled by HAWKEYE at low altitudes outside the plasmapause including the polar cap. The electric ULF noise is composed of a background and intense component which differ in spectral index. The intense electric ULF component coincides with the magnetic ULF noise near the auroral oval and both of these signals correlate with shear in the velocity field which peaks near the auroral zone.

The ULF magnetic noise has the same spectral index and relative location as that reported by D'Angelo et al. [1974] at 3-5 R_e in the polar cusp. Assuming the signals are generated by similar mechanisms scaling arguments are used to test different interpretations of the signals. The results do not support field-aligned currents but do support turbulence models.

The measurements of ULF electric noise by Kelly and Mozer [1972] report a phase velocity much less than the spacecraft velocity. Since the ULF electric noise observed by Kelly and Mozer has similar spectral densities, spectral intensities and location to that reported here, the wave vectors are assumed to be related to the measured frequency by $\bar{k} \cdot \bar{V}_{s/c} = 2\pi f$. Hence power spectral indices for the background and intense electric signal in k-space are 1.89 ± .26 and 2.80 ± .34.

Turbulence in a fluid distributes energy in k-space as a power law. A two-dimensional fluid is characterized by power spectral indices of 5/3 and 3 respectively below and above the wave vector at which the fluid is stirred. In a three-dimensional fluid energy moves only toward larger wave vectors with a power spectral index of 5/3. Velocity shear instabilities are most unstable to perturbations whose wave vector is perpendicular to the ambient magnetic field, and thus, in the region of generation, turbulence should be two dimensional. The observal spectral index of 2.80 ± .34 in the region driven by velocity shear agrees with the two-dimensional theory for wave vectors larger than those exciting the plasma. Outside the region of velocity shear the electric signal is reduced in amplitude and the spectral index is closer to 5/3. Since there is no apparent mechanism to two-dimensionally stir the plasma at wave vectors larger than observed, this may represent three-dimensional turbulence which originated as two-dimensional turbulence in the velocity shear region.

The effect of wind moving across water predicted by the Kelvin-Helmholtz instability is not waves but rather white caps [Chandrashekar, 1961]. The electric measurements presented here are the plasma analogy of white caps.

ACKNOWLEDGEMENTS

I wish to thank D. Gurnett for providing the HAWKEYE-1 VLF experiment data which form the basis of this study. I also wish to thank N. D'Angelo and D. Gurnett for helpful conversations and critical readings of the manuscript. L. Frank and K. Ackerson made the low energy particle data available. R. West and G. Voots assisted in data processing.

This research was supported in part by the National Aeronautics and Space Administration under Contract NAS1-11257 and Grant NGL-16-001-043 (97).

REFERENCES

Batchelor, B. K., The Theory of Homogeneous Turbulence, Cambridge University Press, London, 1970.

Barrington, R. E., T. R. Hartz, and R. W. Harvey, Diurnal distribution of ELF, VLF, and LF noise at high latitudes as observed by Alouette 2, J. Geophys. Res., 76, 5278-5291, 1971.

Carpenter, D. L., Whistler studies of the plasmapause in the magnetosphere, J. Geophys. Res., 71, 693, 1966.

Cauffman, David P., and Donald A. Gurnett, Double-probe measurements of convection electric fields with the Injun-5 satellite, J. Geophys. Res., 76, 6014-6027, 1971.

Chandrasekhar, S., Hydrodynamic and Hydromagnetic Stability, Clarendon Press, Oxford, England, 1961.

D'Angelo, Nicola, Kelvin-Helmholtz instability in a fully ionized plasma in a magnetic field, Phys. Fluids, 8, 1748-1750, 1965.

D'Angelo, N., VLF flunctuations at the polar cusp boundaries, J. Geophys. Res., 78, 1206-1209, 1973.

D'Angelo, N., and S. V. Goeler, Investigation of the Kelvin-Helmholtz instability in a cesium plasma, Phys. Fluids, 9, 309-313, 1966.

D'Angelo, N., A. Bahnsen, and H. Rosenbauer, Wave and particle measurements at the polar cusp, J. Geophys. Res., 79, 3129-3134, 1974.

Frank, L. A., Plasma in the earth's polar magnetosphere, J. Geophys. Res., 76, 5202-5219, 1971.

Gerwin, Richard A., Stability of the interface between two fluids in relative motion, Reviews of Modern Physics, 40, 652-658, 1968.

Gurnett, D. A., and L. A. Frank, ELF noise bands associated with auroral electron precipitation, J. Geophys. Res., 77, 3411-3417, 1972.

Hasegawa, Akira, Plasma Instabilities and their Non-linear Effects, Springer-Verlang, New York, 1975.

Heppner, J. P., Polar-cap electric field distributions related to the interplanetary magnetic field direction, J. Geophys. Res., 77, 4877-4887, 1972.

Kelley, M. C., and F. S. Mozer, A satellite survey of vector electric fields in the ionosphere at frequencies of 10 to 500 Hz, J. Geophys. Res., 77, 4158-4173, 1972.

Kintner, P., K. Ackerson, L. Frank, and D. Gurnett, Correlated electric field and particle observations at the low altitude polar cusp, U. of Iowa Research Report, in preparation, 1976.

Kraichnan, Robert H., Inertial ranges in two-dimensional turbulence, Phys. Fluids, 10, 1417-1423, 1967.

Kurth, William S., Mark M. Baumback, and Donald A. Gurnett, Direction-finding measurements of auroral kilometric radiation, J. Geophys. Res., 80, 2764-2770, 1975.

Laaspere, T., W. C. Johnson, and L. C. Semprebon, Observations of auroral hiss, LHR noise and other phenomena in the frequency range 20 Hz - 540 kHz on OGO 6, J. Geophys. Res., 76, 4477-4493, 1971.

Lanzerotti, L. J., A. Hasegawa, and N. A. Tartaglia, Morphology and interpretation of magnetospheric plasma waves at conjugate points during December solstice, J. Geophys. Res., 77, 6731-6745, 1972.

Lilly, Douglas K., Numerical simulation of two-dimensional turbulence, Phys. Fluids Supplement II, 10, 240-249, 1969.

Maynard, N. C., and J. P. Heppner, Variations in electric fields from polar orbiting satellites, Goddard Space Flight Center report X-612-69-374, Greenbelt, Maryland.

Muzzio, J. L. R., and Jacyntho J. Angerami, OGO 4 observations of extremely low frequency hiss, J. Geophys. Res., 77, 1157-1173, 1972.

Russel, Christofer T., Charles R. Chappell, Michel D. Montgomery, Marcia Neugebauer, and Fredrick L. Scarf, OGO 5 observations of the polar cusp on November 1, 1968, J. Geophys. Res., 76, 6743-6764, 1971.

Samson, J. C., J. A. Jacobs, and G. Rostokev, Latitude-dependent characteristics of long-period geomagnetic micropulsations, J. Geophys. Res., 76, 3675-3683, 1971.

Shoucri, Magdi M., Linear istabilities in the quasistatic guiding-center plasma, Thesis, University of Iowa, Iowa City, Iowa, 1974.

Southwood, D. J., The hydromagnetic stability of the magnetospheric boundary, Planet. Space Sci., 16, 587-605, 1968.

FIGURE CAPTIONS

Figure 1 The output of the electric and magnetic receivers from 1.7 Hz to 5.6 kHz during a portion of the HAWKEYE-1 orbit beginning near the magnetic equator and ending over the polar cap with the loss of telemetry coverage. Each frequency is displayed from 0 volts to 5 volts representing 100 dB of amplitude.

Figure 2 A survey of the ULF magnetic noise at 5.6 Hz exceeding a threshold of 2×10^{-4} gamma^2/Hz shown in invariant latitude and magnetic local time. Each dot represents one measurement. The dashed line is the equatorward border of the Feldstein $K_p = 1$ auroral oval. The cross hatched area was not sampled by HAWKEYE-1.

Figure 3 Four magnetic spectral densities for 1.7 Hz, 5.6 Hz, 17 Hz, and 56 Hz during the period 2243 UT to 2245 UT on Day 263, 1974.

Figure 4 Histogram of magnetic power spectral indices.

Figure 5 A survey of the ULF electric noise at 17 Hz exceeding a threshold of $2 \times 10^{-10}\ V^2/m^2$ Hz shown in invariant latitude and magnetic local time. Each dot represents one measurement. The dashed line is the plasmapause position for $K_p = 2\text{-}4$. The crosshatched area was not sampled by HAWKEYE-1.

Figure 6 Electric spectral densities for 1.7 Hz, 5.6 Hz, 17 Hz and 56 Hz. The left panel contains measurements of the intense signal from 2244 UT to 2246 UT, Day 263, 1974. The right panel contains measurements of the background signals from 2240 UT to 2242 UT.

Figure 7 Electric power spectral indices separated into intense and background signals at $E_o^2 = 2 \times 10^{-7}\ V^2/m^2$ Hz.

Figure 8 Convection velocity vectors plotted from the HAWKEYE-1 location in magnetic local time and invariant latitude.

Figure 9 The magnetic and electric power spectral densities from 1.7 Hz to 56 Hz in the lower two panels and the convection velocity measurements and velocity shear in the upper two panels for Day 263, 1974.

Figure 10 The same format as Figure 9 for Day 234, 1974.

Figure 11 Magnetic spectral densities for 1.7 Hz, 5.6 Hz, 17 Hz, and 56 Hz during the peak amplitudes on 4 different days.

Figure 12 An example of the effect of velocity shear on a magnetic field line.

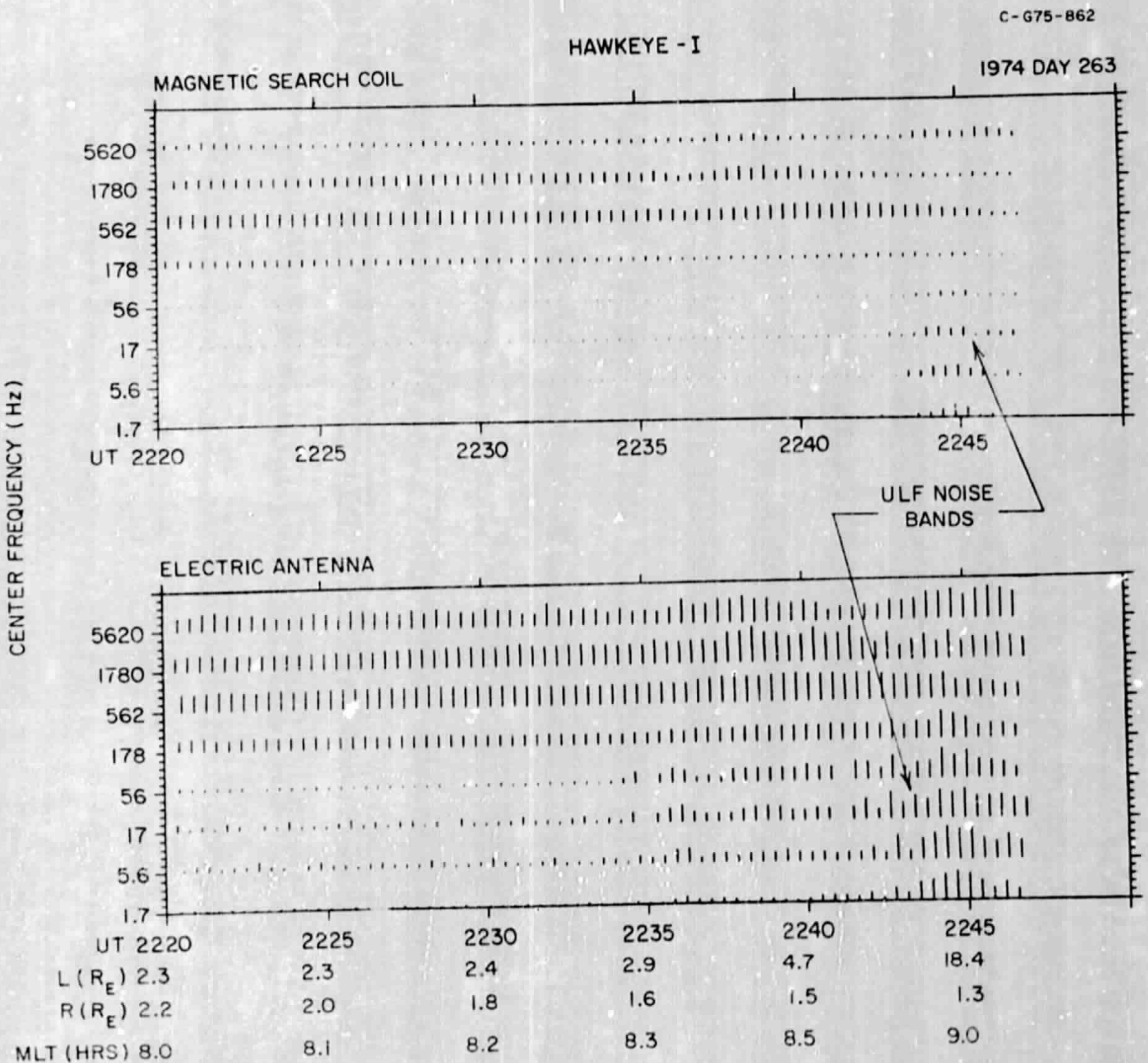
C-G75-862
HAWKEYE - I
1974 DAY 263
MAGNETIC SEARCH COIL
5620
1780
562
178
56
17
5.6
1.7
UT 2220
2225
2230
2235
2240
2245
CENTER FREQUENCY (Hz)
ULF NOISE
BANDS
ELECTRIC ANTENNA
5620
1780
562
178
56
17
5.6
1.7
UT 2220
2225
2230
2235
2240
2245
L (R_E) 2.3
2.3
2.4
2.9
4.7
18.4
R (R_E) 2.2
2.0
1.8
1.6
1.5
1.3
MLT (HRS) 8.0
8.1
8.2
8.3
8.5
9.0

Figure 1

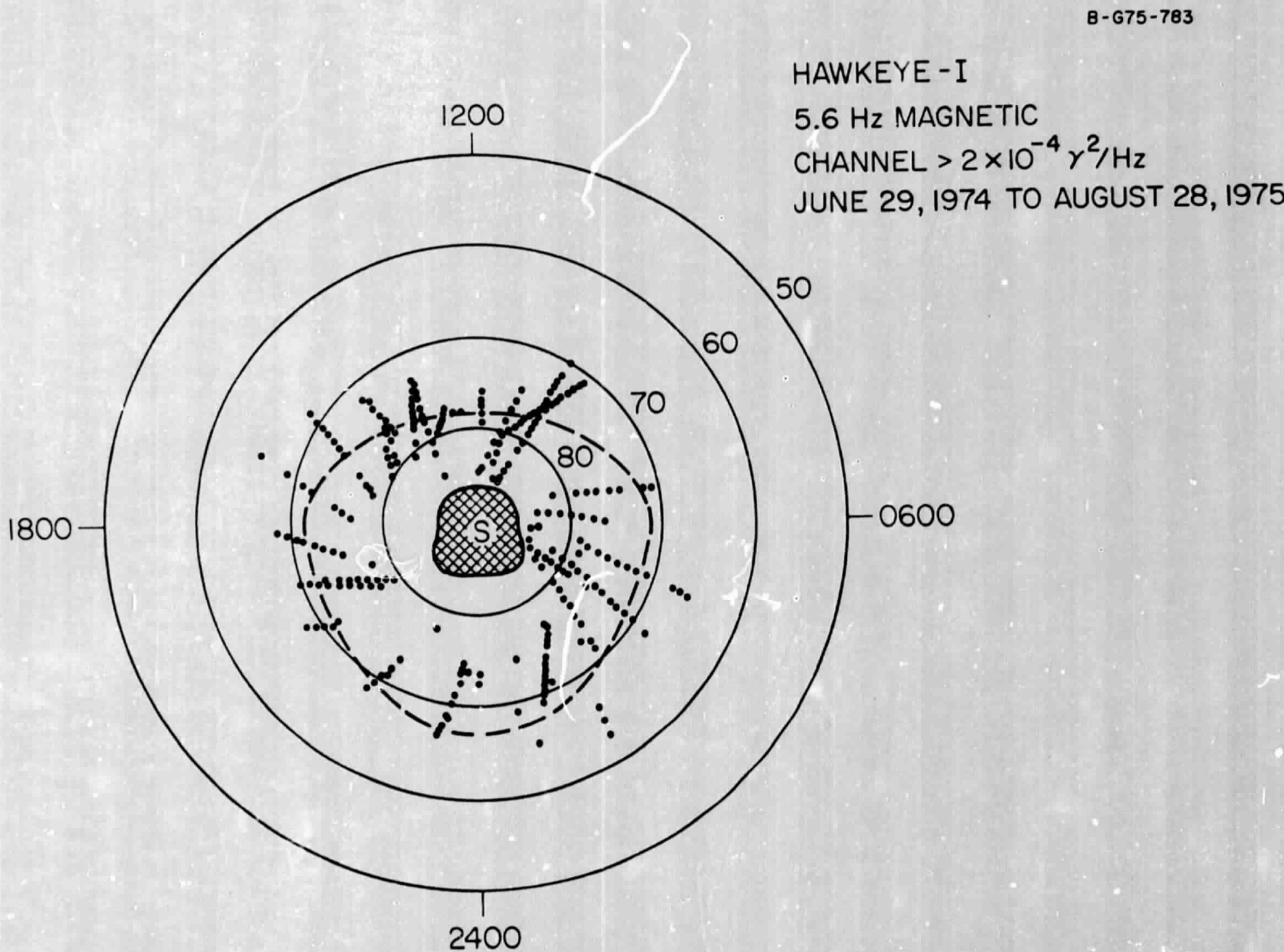
B-G75-783
HAWKEYE-I
5.6 Hz MAGNETIC
CHANNEL > $2 \times 10^{-4}\ \gamma^2/\mathrm{Hz}$
JUNE 29, 1974 TO AUGUST 28, 1975
1200
0600
1800
2400
50
60
70
80
S

Figure 2

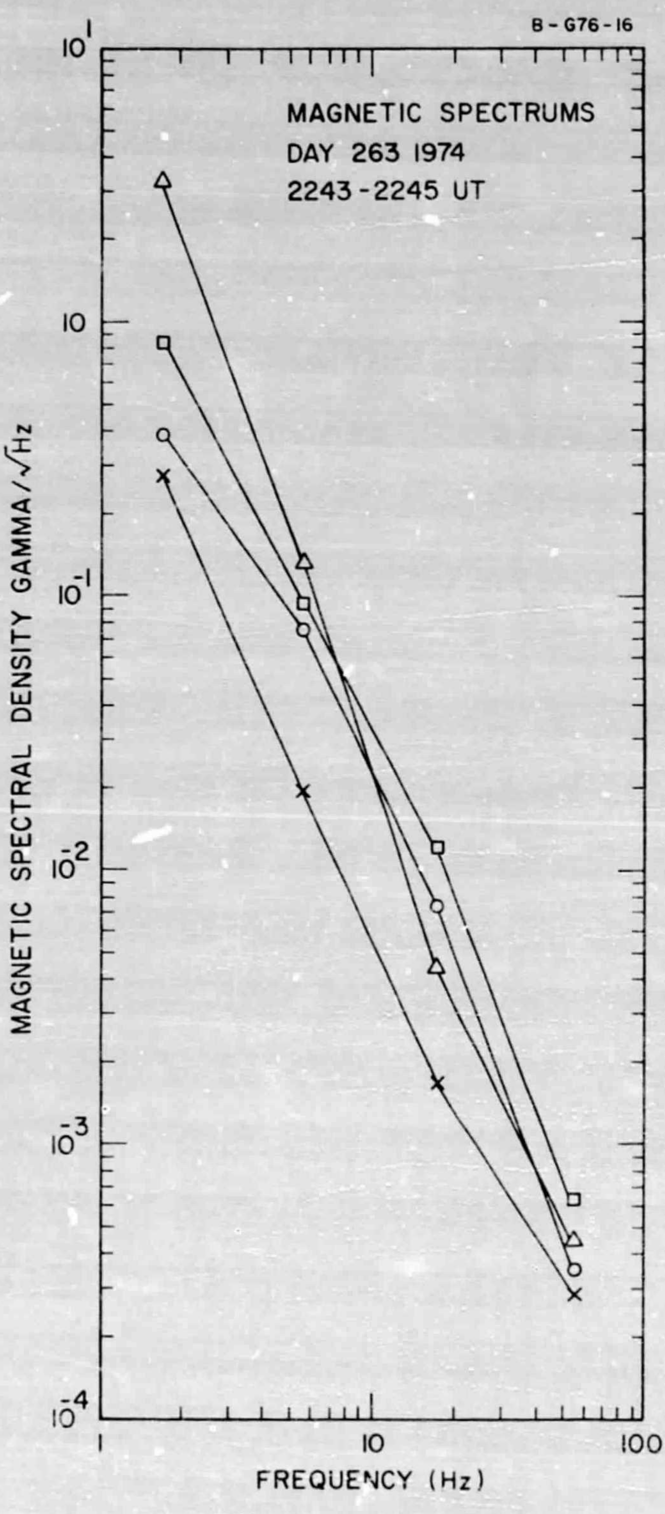
B - G76 - 16
MAGNETIC SPECTRUMS
DAY 263 1974
2243 - 2245 UT
MAGNETIC SPECTRAL DENSITY GAMMA/√Hz
FREQUENCY (Hz)
10
100
1

Figure 3

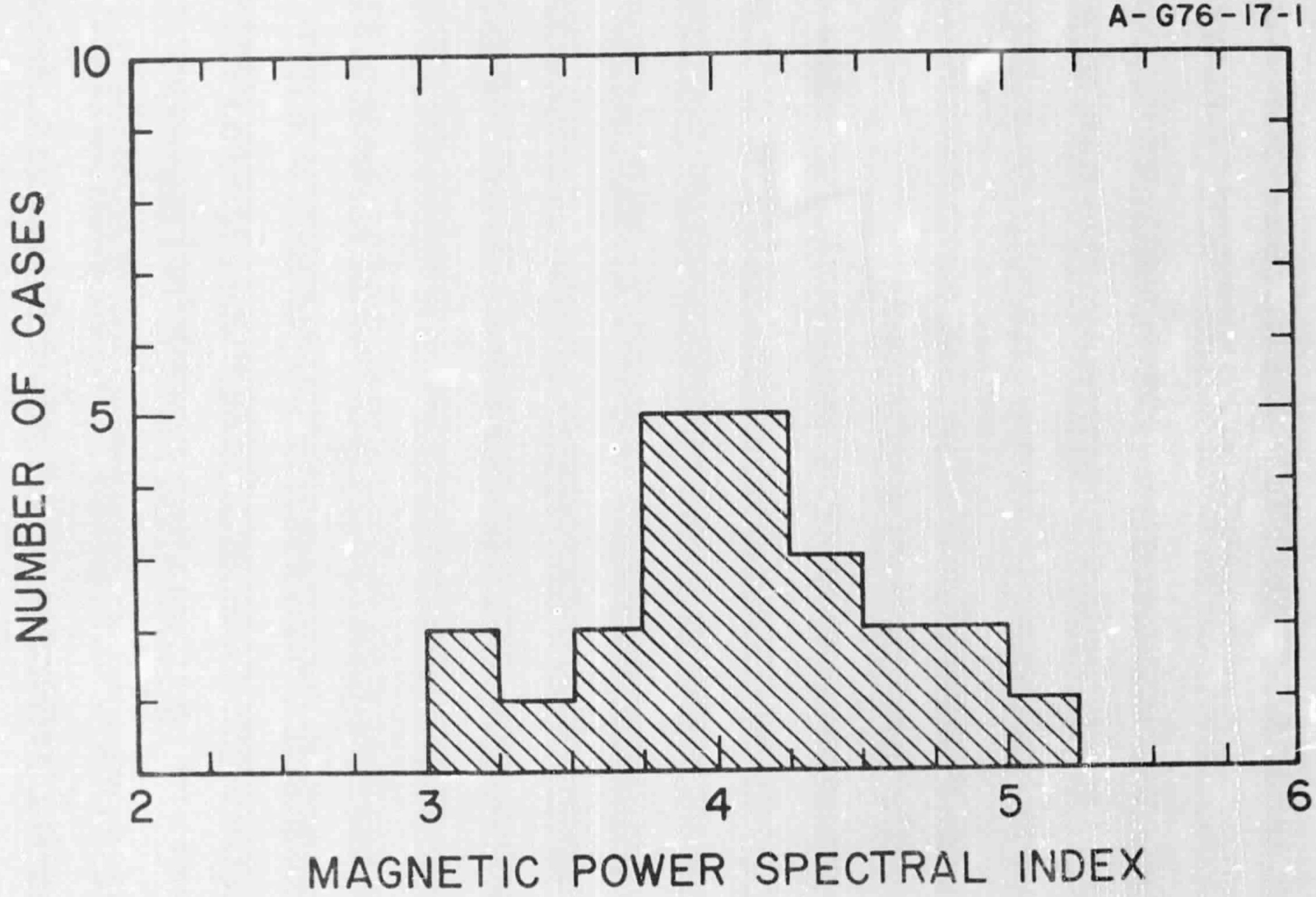
A-G76-17-1
10
5
NUMBER OF CASES
2
3
4
5
6
MAGNETIC POWER SPECTRAL INDEX

Figure 4

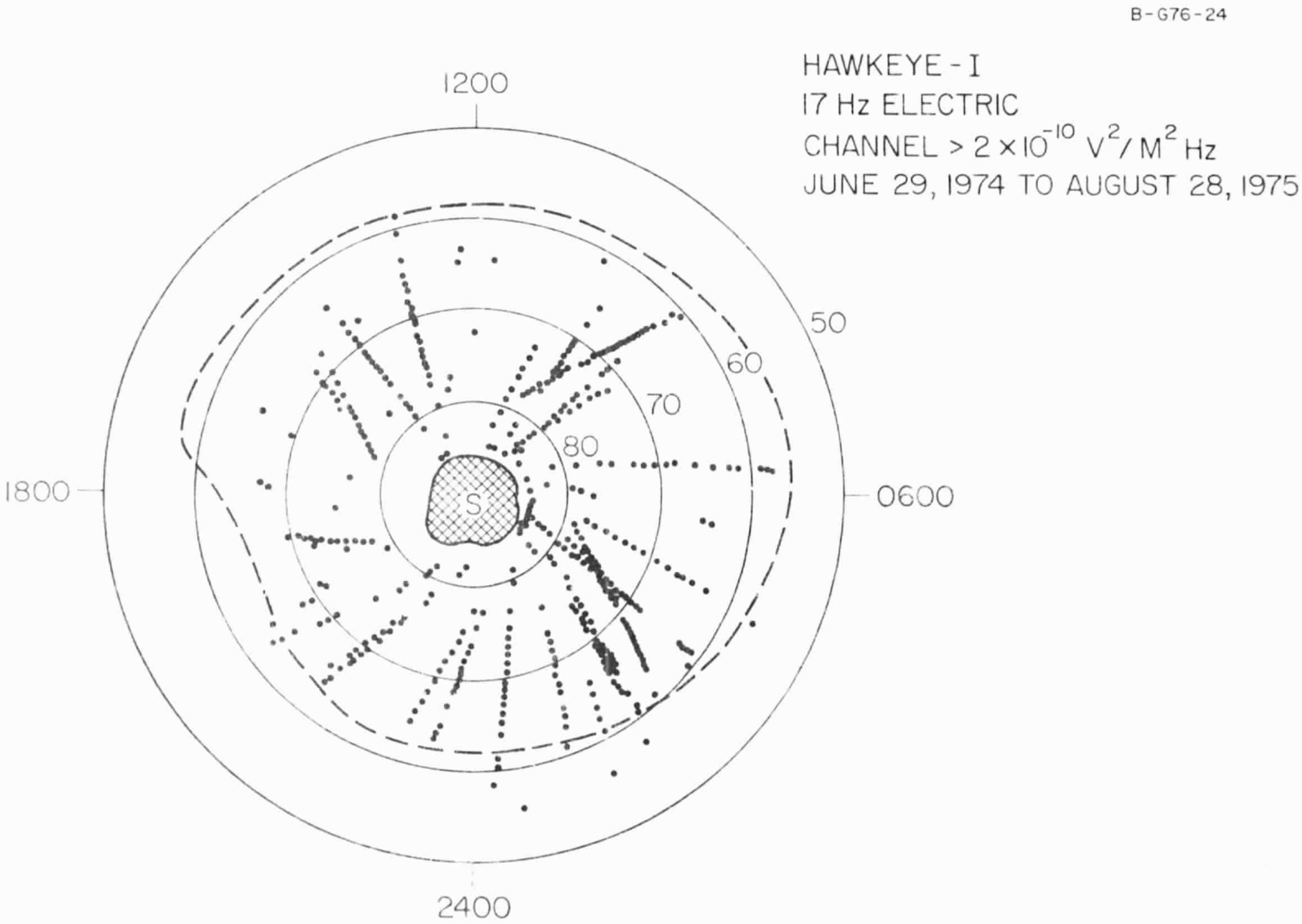
B-G76-24
HAWKEYE - I
17 Hz ELECTRIC
CHANNEL > 2 × 10^{-10} V^2/M^2 Hz
JUNE 29, 1974 TO AUGUST 28, 1975
1200
1800
0600
2400
50
60
70
80
S

Figure 5

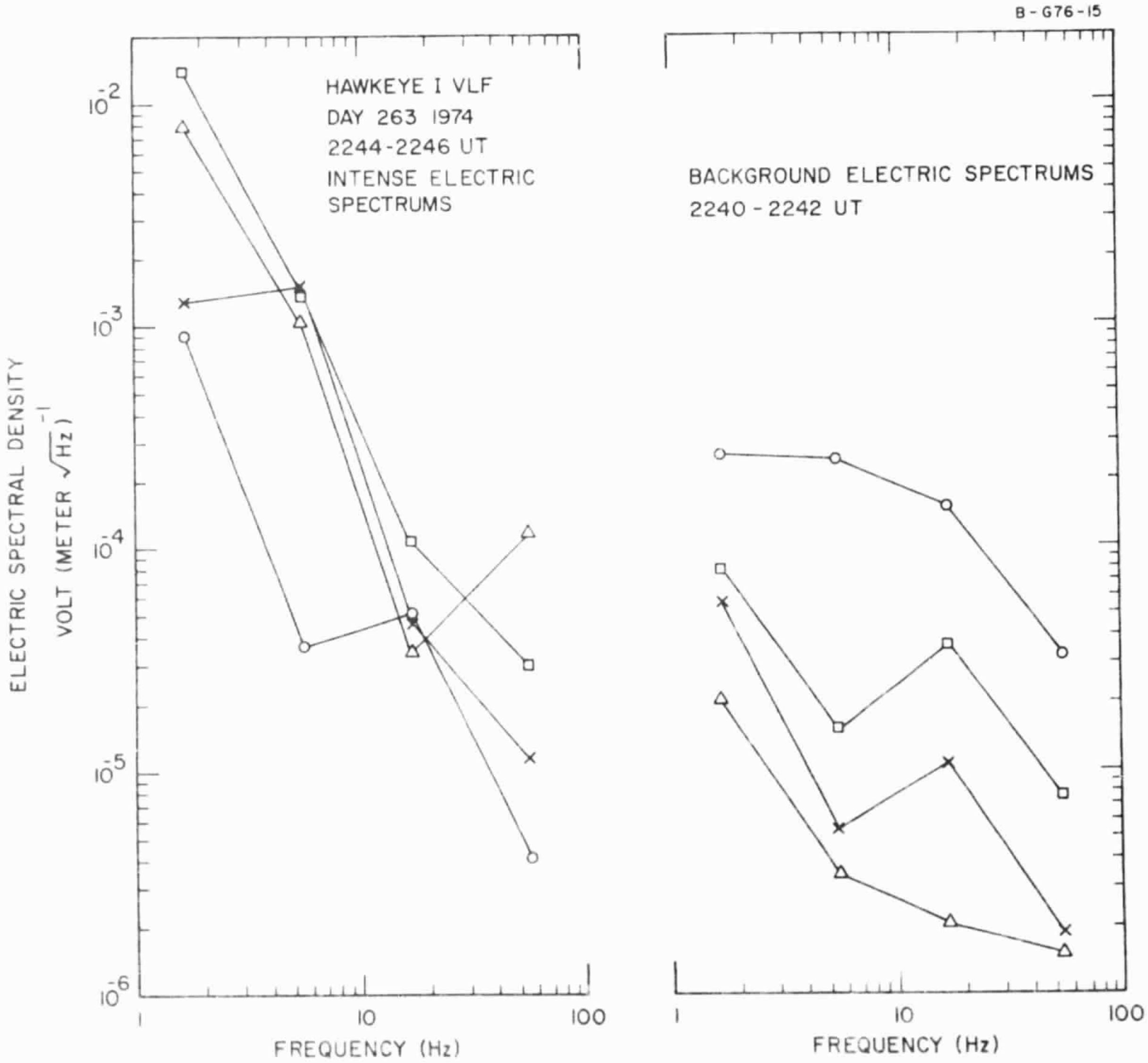
B-G76-15
HAWKEYE I VLF
DAY 263 1974
2244-2246 UT
INTENSE ELECTRIC
SPECTRUMS
BACKGROUND ELECTRIC SPECTRUMS
2240-2242 UT
ELECTRIC SPECTRAL DENSITY
VOLT (METER √Hz)^-1
10^-2
10^-3
10^-4
10^-5
10^-6
1
10
100
FREQUENCY (Hz)
1
10
100
FREQUENCY (Hz)

Figure 6

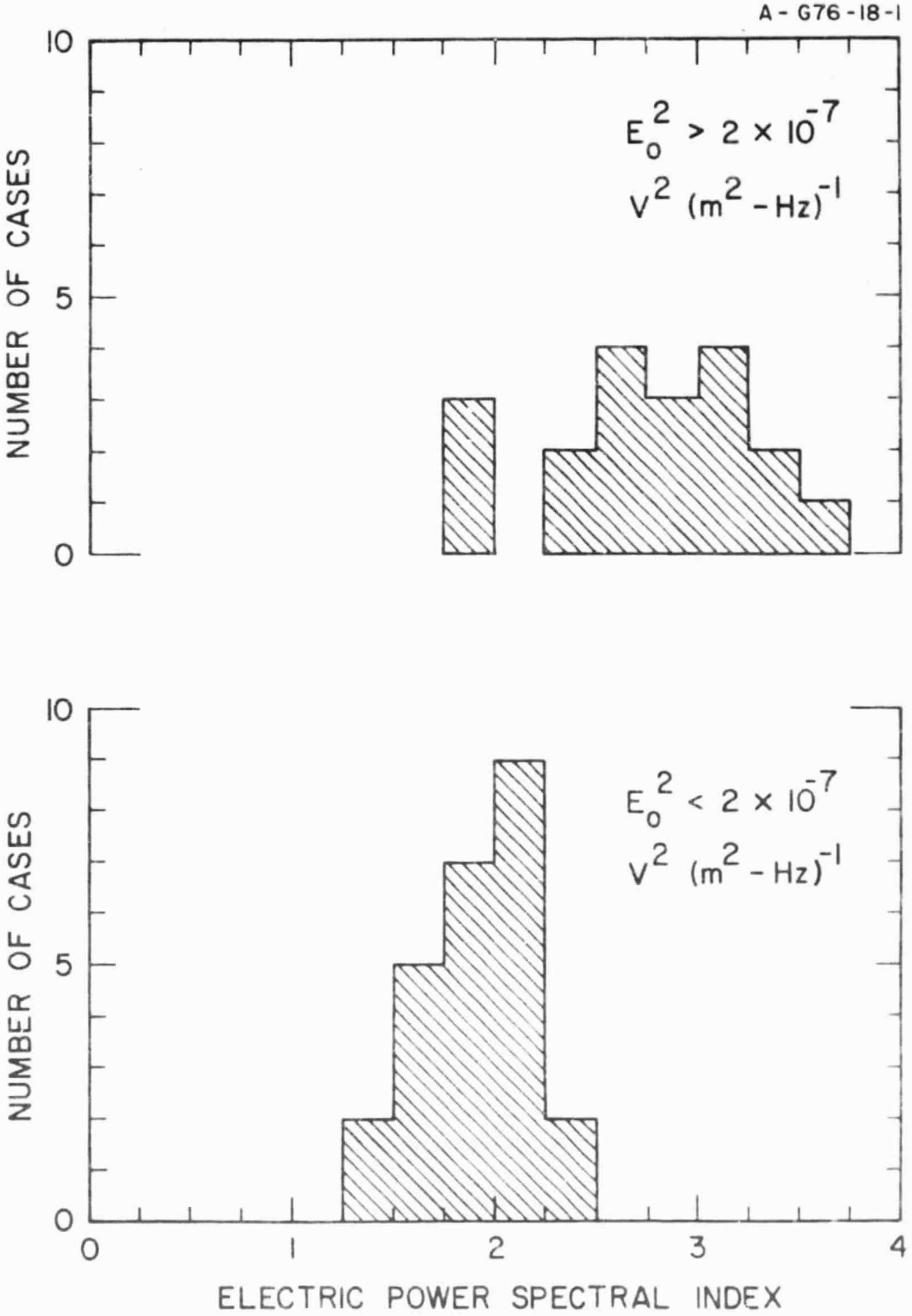
A - G76 - 18 - 1
NUMBER OF CASES
$E_o^2 > 2 \times 10^{-7}$
$V^2 (m^2 - Hz)^{-1}$
$E_o^2 < 2 \times 10^{-7}$
$V^2 (m^2 - Hz)^{-1}$
ELECTRIC POWER SPECTRAL INDEX

Figure 7

B-G75-307

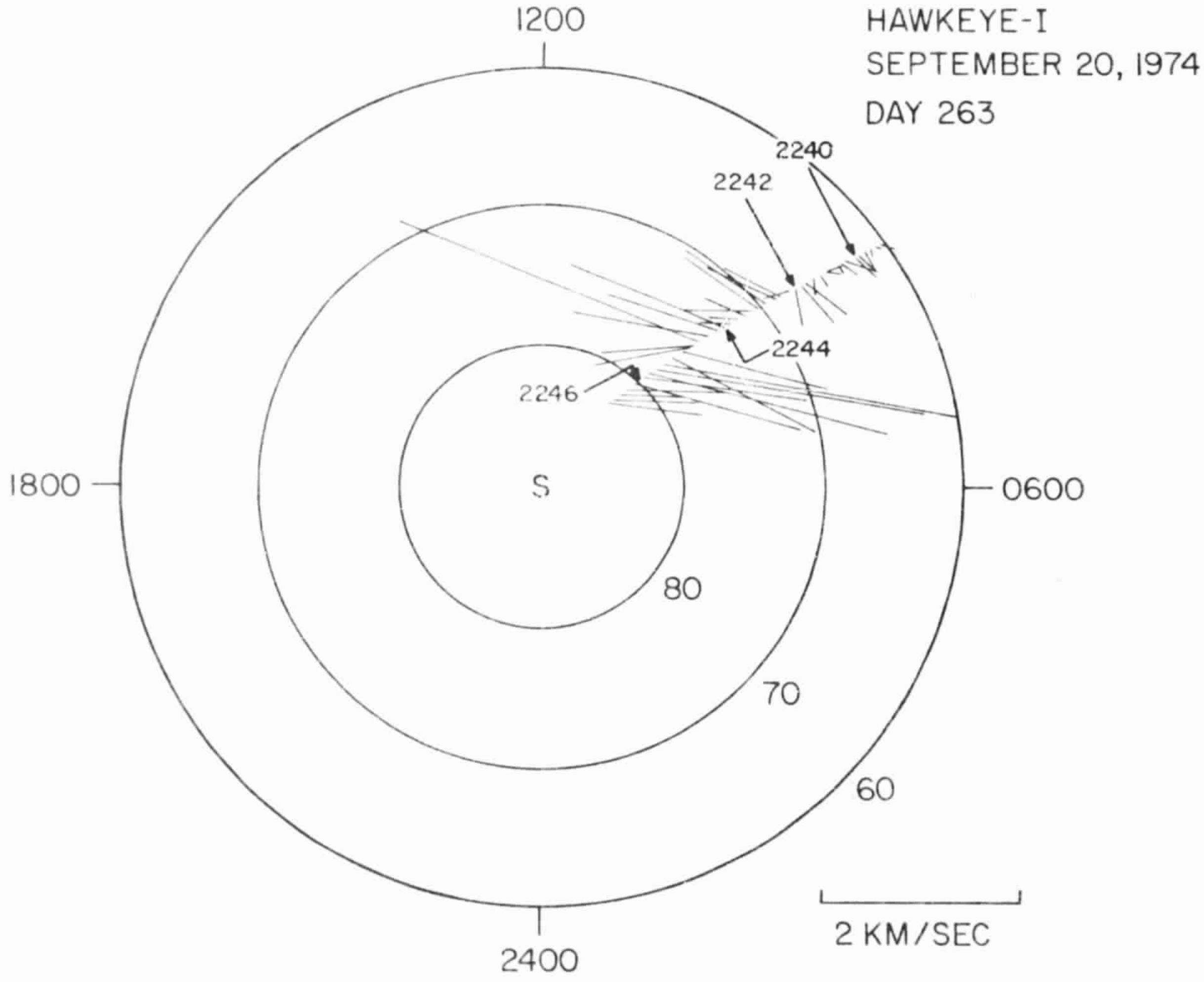

Figure 8

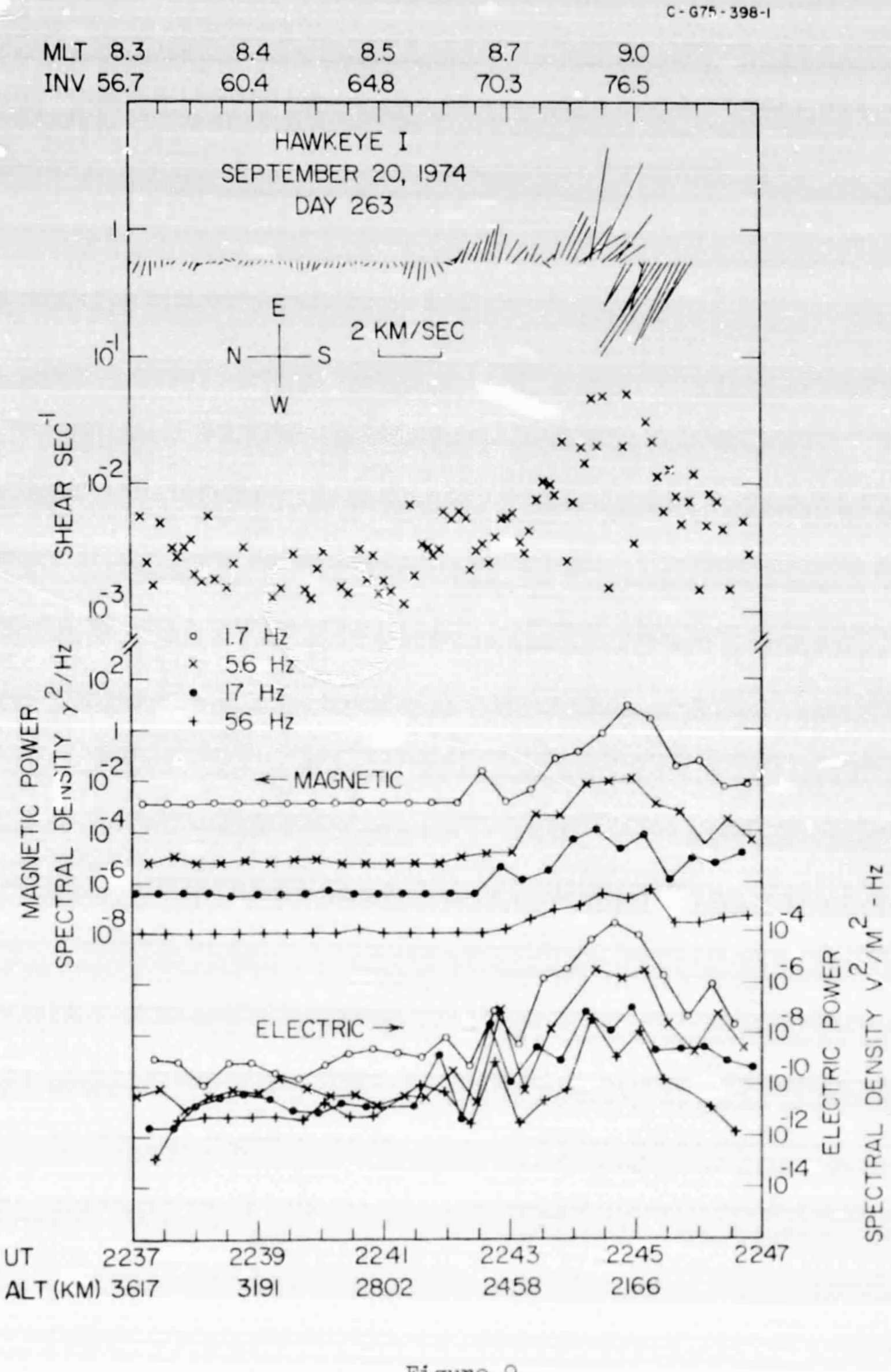
C-G75-398-1
MLT 8.3 8.4 8.5 8.7 9.0
INV 56.7 60.4 64.8 70.3 76.5
HAWKEYE I
SEPTEMBER 20, 1974
DAY 263
2 KM/SEC
E
N S
W
SHEAR SEC^{-1}
1
10^{-1}
10^{-2}
10^{-3}
1.7 Hz
5.6 Hz
17 Hz
56 Hz
MAGNETIC POWER SPECTRAL DENSITY γ^2/Hz
10^2
1
10^{-2}
10^{-4}
10^{-6}
10^{-8}
← MAGNETIC
ELECTRIC →
ELECTRIC POWER SPECTRAL DENSITY V^2/M^2-Hz
10^{-4}
10^{-6}
10^{-8}
10^{-10}
10^{-12}
10^{-14}
UT 2237 2239 2241 2243 2245 2247
ALT (KM) 3617 3191 2802 2458 2166

Figure 9

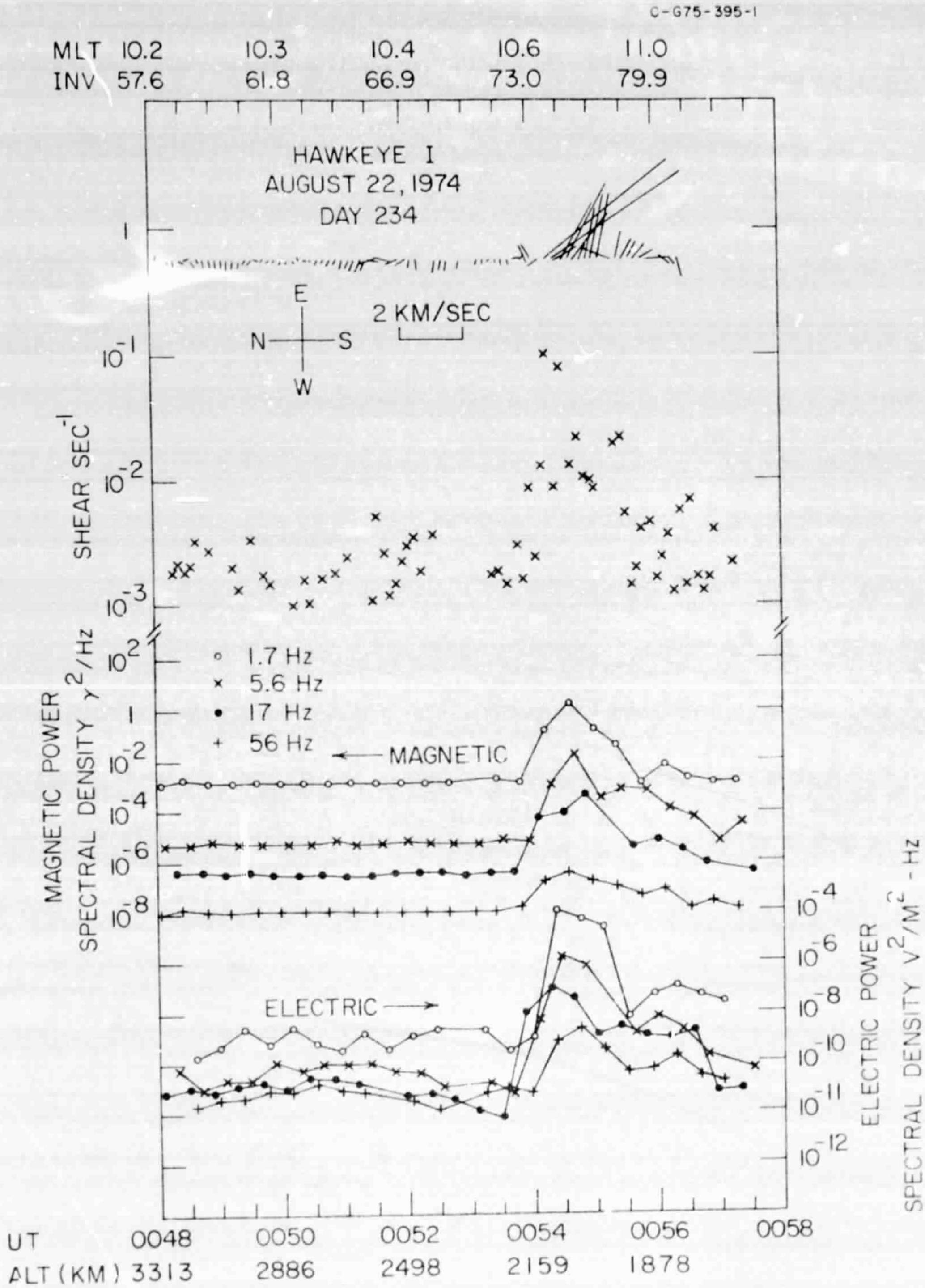
C-G75-395-1
MLT 10.2 10.3 10.4 10.6 11.0
INV 57.6 61.8 66.9 73.0 79.9
HAWKEYE I
AUGUST 22, 1974
DAY 234
2 KM/SEC
E
N
S
W
SHEAR SEC^{-1}
MAGNETIC POWER SPECTRAL DENSITY γ^2/Hz
1.7 Hz
5.6 Hz
17 Hz
56 Hz
MAGNETIC
ELECTRIC
ELECTRIC POWER SPECTRAL DENSITY V^2/M^2 - Hz
UT 0048 0050 0052 0054 0056 0058
ALT (KM) 3313 2886 2498 2159 1878

Figure 10

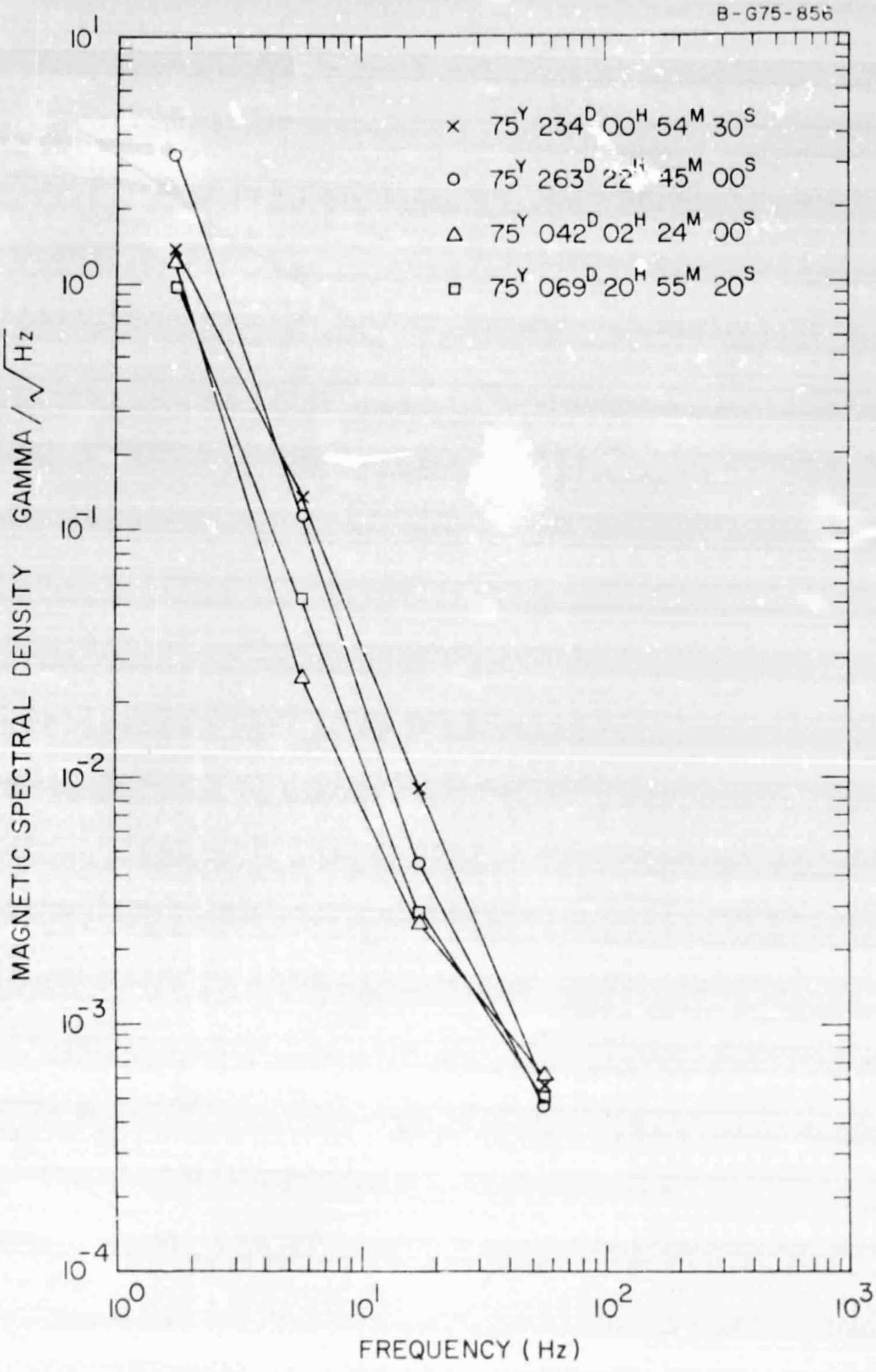
B-G75-856
75Y 234D 00H 54M 30S
75Y 263D 22H 45M 00S
75Y 042D 02H 24M 00S
75Y 069D 20H 55M 20S
MAGNETIC SPECTRAL DENSITY GAMMA/√Hz
FREQUENCY (Hz)

Figure 11

A-G76-23

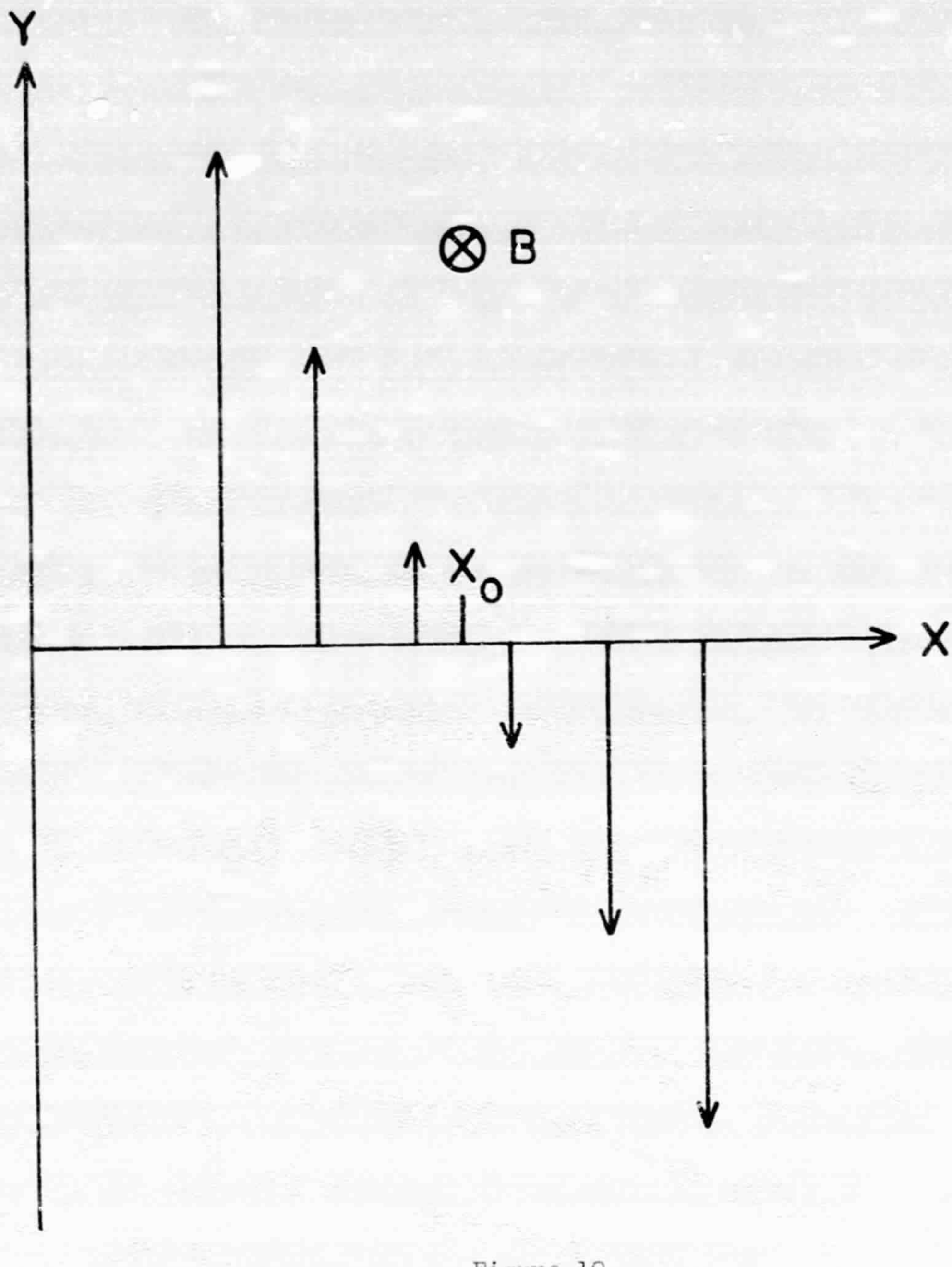

Figure 12